Raman amplification in the coherent wave-breaking regime

J. P. Farmer and A. Pukhov
Theoretische Physik I, Heinrich Heine Universität, 40225 Düsseldorf, Germany
(Received 8 September 2015; published 21 December 2015)

In regimes far beyond the wave-breaking threshold of Raman amplification, we show that significant amplification can occur after the onset of wave breaking, before phase mixing destroys the coherent coupling between pump, probe, and plasma wave. Amplification in this regime is therefore a transient effect, with the higher-efficiency "coherent wave-breaking" (CWB) regime accessed by using a short, intense probe. Parameter scans illustrate the marked difference in behavior between below wave breaking, in which the energy-transfer efficiency is high but total energy transfer is low, wave breaking, in which efficiency is low, and CWB, in which moderate efficiencies allow the highest total energy transfer.

DOI: 10.1103/PhysRevE.92.063109 PACS number(s): 52.38.Bv, 52.35.−g

I. INTRODUCTION

Raman amplification in plasma has been suggested as a mechanism to allow the creation of ultrashort, ultraintense laser pulses, [1] which have applications across science and technology. Using plasma as a gain medium offers the advantage that, unlike solid-state media, it does not have a damage threshold, potentially reducing or removing the need for stretching and compression of the laser pulse, allowing either a reduction in size or an increase in power of next-generation laser systems.

In the Raman interaction, a probe pulse interacts with a counterpropagating pump, driving a plasma wave through the ponderomotive force of their beat. If the pump and probe frequencies, ω_a and ω_b, are chosen such that the probe is downshifted from the pump by the plasma frequency, ω_p, the plasma wave is resonantly excited and may grow to large amplitude. The resulting density perturbation acts as a moving Bragg grating, which serves to scatter and Doppler shift the pump pulse into the probe, amplifying the latter.

Although the plasma itself does not have a damage threshold, there remain several effects which act to limit the interaction, such as filamentation and parasitic spontaneous backscatter of the pump [2]. Further, the high wave number and low phase velocity of the laser beat, which allows a large-amplitude plasma wave to be excited, means that the plasma wave can break for even moderate laser intensities, $\ll 1 \times 10^{18}$ W cm^{-2} [3], leading to strong damping [4], which will limit the coupling between pump and probe [5].

These effects likely contribute to the low efficiencies reported by experimental campaigns [6–9], the best to date being by Ren *et al.*, achieving 6.4% in a double-pass setup [10]. Previous theoretical and computational works have focused on the optimal pump amplitude for efficient amplification [2,5,11,12]. Although it is known that the highest efficiencies are achieved below the wave-breaking threshold, the necessarily low intensities would require large interaction volumes to scale to high power. In this work we therefore focus on the energy-transfer efficiency far beyond the wave-breaking threshold.

It is interesting to note, however, that simulations carried out in this regime have yielded significantly different efficiencies, even for similar parameters, ranging from 35% in the work of Trines *et al.* [2] to less than 10% in that of Toroker *et al.* [11]. These apparently contradictory results have been the subject of significant discussion [11,12], although the main cause has not previously been identified. Clearly, reconciling the differences between simulations is important if reliable comparison to experiment is to be made.

In this work we identify a new process in the Raman interaction, coherent wave breaking. In Sec. II we illustrate a strong dependence of the energy-transfer efficiency on the probe duration, which explains the difference between efficiencies observed in other works. A simple analytical model is developed in Sec. III, allowing the relevant physical processes to the identified. Section IV discusses the applicability of the results to experiments, and conclusions are drawn in Sec. V.

II. INFLUENCE OF PROBE DURATION FAR BEYOND THE WAVE-BREAKING LIMIT

We make use of the Leap code [13], which is based on a laser-envelope particle-in-cell model. Since the Raman interaction is predominantly planar due to the short wavelength of the excited plasma wave and the relatively large interaction cross section, we here limit ourselves to one-dimensional (1D) simulations. In addition to a low computational overhead, this geometry has the further advantage that the plasma response modeled by the Leap code is exact [14]. Although multidimensional simulations are certainly important for direct comparison to experiments, the fundamental processes are often obfuscated, as different regimes of amplification may be in effect at different radii, discussed in more detail in Sec. IV. We therefore make use of 1D simulations in order to characterize the coherent wave-breaking regime of interest here.

Figure 1 shows the evolution of the probe pulse for different initial probe durations. Gaussian pulses are used, with FWHM-intensity durations of 17, 50, and 83 fs. A flat-top, 800 nm pump with duration 30 ps and intensity 1×10^{15} W cm^{-2} is used to amplify a probe with initial intensity 1×10^{16} W cm^{-2} in a plasma of density 4.4×10^{18} cm^{-3} with an initial temperature of 10 eV. This corresponds to $\omega_a/\omega_p = 20$, $\omega_b/\omega_p = 19$ and a pump intensity 30 times above the threshold for wave breaking to occur [3]. These are the same parameters as used by Toroker *et al.* [11] in their investigation of the strong-wave-breaking regime, with the longest pulse used here equivalent to the probe used in that work. Although the longer pump length used here (30 ps compared to ∼1 ps) would result in higher plasma temperatures, we retain the

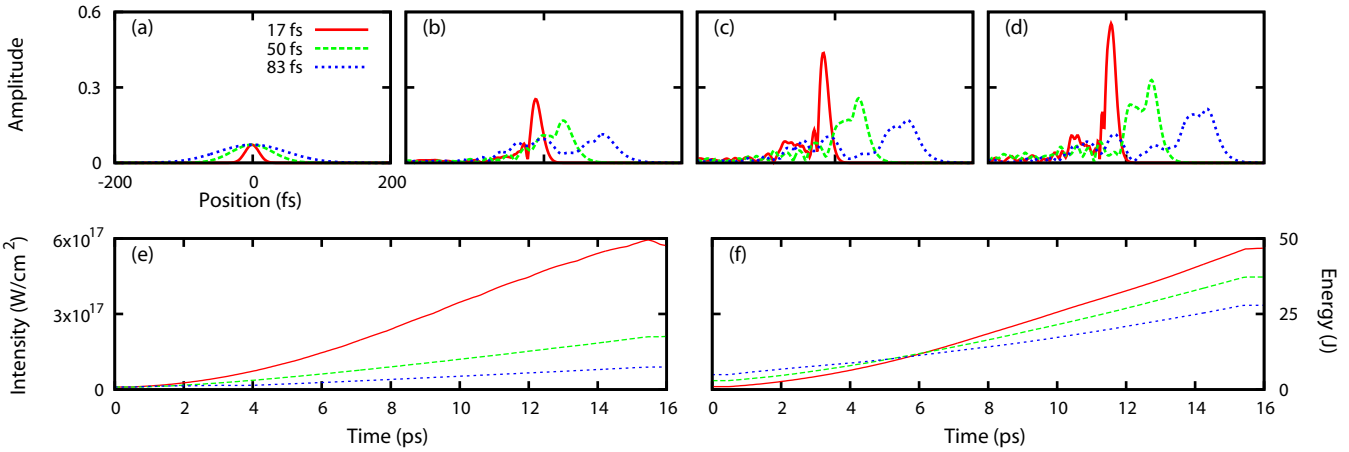

FIG. 1. (Color online) Plots showing evolution of the probe pulse for three different initial durations. (a–d) Snapshots of the amplitude at 0.5, 5.5, 10.5, and 15.5 ps. (e) Peak probe intensity against time. (f) Total probe energy against time.

10 eV temperature to allow direct comparison to those results. This longer pump allows comparison with the results of Trines *et al.*

Figures 1(a)–1(d) show snapshots of the probe profiles at different times during the interaction, given as the reduced vector potential $eE/mc\omega_b$, with E the electric field amplitude, c the vacuum speed of light, and $-e$ and m the electron charge and mass. It can be seen that in all cases the probe is amplified and compressed. However, as highlighted in Fig. 1(e), the greatest amplification is achieved for the shortest pulse, which reaches an intensity of 6×10^{17} W cm^{-2}. The reduction in peak intensity at the end of the simulation is due to dispersion as the probe continues to propagate through plasma after the end of the pump at 15.5 ps. Energies were calculated by scaling to three dimensions, taking a pulse radius (e-squared-folding distance) of 595 μm, equal to that used by Trines *et al.* [2], and are shown in Fig. 1(f). While the 17 fs probe is initially the least energetic and is compressed to 9.7 fs during amplification, it goes on to exceed the energy of the longer pulses. The total pump energy for these parameters is 166 J, giving pump-to-probe energy-transfer efficiencies over the full interaction for the three probe durations of, from shortest to longest, 28%, 21%, and 14%.

We note from Fig. 1(f) that the growth of the probe energy is better than linear, with the efficiency increasing over the interaction as the probe becomes more intense. The gain of 23 J over a 30 ps pump observed for the 83 fs probe is therefore consistent with the results of Toroker *et al.*, which for this pulse width correspond to an energy transfer of $\sim$0.5 J over $\sim$1 ps pump. Trines *et al.* used similar parameters to the 50 fs probe used here, but with cold plasma and an on-axis intensity for pump and probe double that used here. However, even with those factors taken into account, the amplification here remains somewhat lower than observed in that work. This disparity could be a result of the initial pulse shape: using a pulse profile with a finite support, for example truncating a Gaussian at 2σ, increases the amplification, giving comparable results.

The improved amplification observed for shorter probe pulses and the sensitivity to the pulse shape are linked to self-steepening, which causes the peak of the amplified pulse to move forward, away from the initial maximum. The effective seed amplitude is therefore reduced, as a point on the leading edge of the initial pulse becomes the seed for amplification, rather than than the peak.

Self-steepening in the Raman process can arise due to many different effects, such as ponderomotive nonlinearity [1], pump depletion [3], and the use of a chirped pump [15], while the presence of a prepulse can lead to superluminous precursors [16]. The self-steepening observed here is a result of wave breaking, as can be seen in Fig. 2. Snapshots of the interaction 1.2 ps into the simulation, before significant amplification occurs, show the pump, probe, and plasma-wave amplitude, the electron phase space and the electron density. The plasma wave amplitude is here given as the absolute value of the coupling susceptibility [13] normalized to the square of the plasma frequency, $|\tilde{\psi}|/\omega_p^2 = |< (n/\gamma n_0)\, e^{i(\phi_a - \phi_b)} >|$, where $\phi_{a,b}$ are the vacuum phases of the pump and probe, n and n_0 are the local and equilibrium plasma electron densities, and γ the plasma-electron Lorentz factor. This value represents the coupling between pump and probe. From linear theory [4], wave breaking occurs when the electron velocity exceeds the phase velocity of the wave, $v_{\rm br}/c \approx \omega_p/2\omega_a = 0.025$, corresponding to $|\tilde{\psi}|/\omega_p^2 = 0.5$.

For the longer pulses, wave breaking occurs on the leading edge of the probe. As a result, phase mixing of the plasma wave has already set in by the time the probe peak is reached, as seen in Fig. 2(d). The resulting density perturbation, shown in Fig. 2(e), loses its periodic structure and no longer efficiently scatters the pump into the probe, lowering amplification.

Although the electrons periodically rephase as they make synchrotron-like oscillations in the broken wave, the shift in resonance means that these plasma echoes have the wrong phase to coherently scatter the pump into the probe. Amplification therefore depends on the coupling susceptibility prior to phase mixing. For the shortest pulse in Fig. 2, the first peak in the coupling susceptibility almost coincides with the peak of the probe, maximising the energy transfer.

If the probe is too short, however, peak amplification may occur behind the probe peak, again lowering energy transfer. This is in fact the case for the 17 fs probe for time $<$1.2 ps, giving a lower energy-transfer rate than observed for the 83 fs

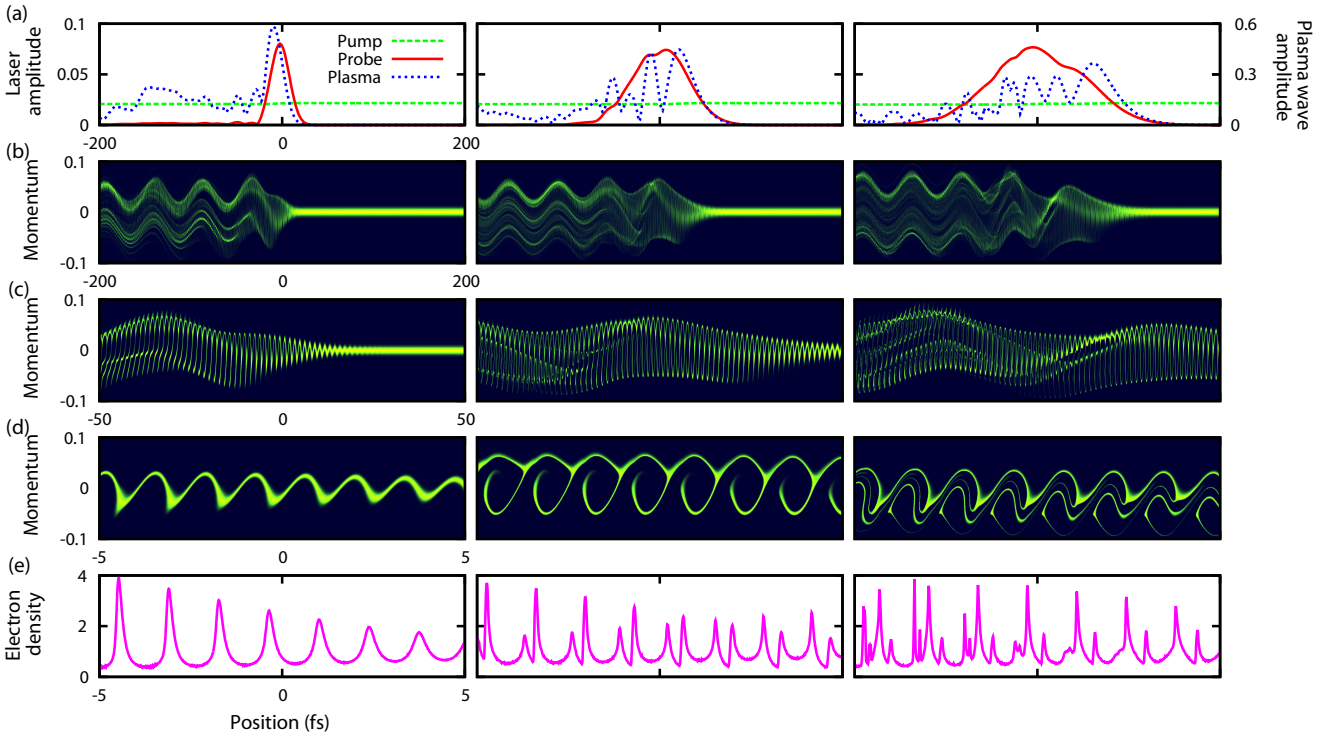

FIG. 2. (Color online) Snapshot of the Raman interaction at time 1.2 ps for initial probe durations of (from left to right) 17, 50, and 83 fs. (a) The pump and probe amplitudes and the effective coupling between the two. (b–d) plots of the electron phase space on different scales, showing (b) the long-wavelength oscillation excited by the breaking plasma wave, (c) the onset of wave breaking itself ($v_{\rm br} \approx 0.025c$), and (d) the electron phase space at the probe peak. (e) The corresponding electron density at the probe peak.

probe. However, as the probe is amplified, the point at which wave breaking occurs moves forward. This causes the point of peak coupling to advance, leading to improved overlap with the probe, increasing energy transfer. From 1.2 ps onwards, the energy-transfer rate is highest for the 17 fs probe, which goes on to become the most energetic after ∼5.5 ps.

In addition to the short-wavelength excitation, $\sim(\pi c/\omega_a)$, driven by the beat of the pump and probe, it is interesting to note that there is a long-wavelength excitation, $\sim(2\pi c/\omega_p)$, as seen in Fig. 2(b). This is not a wake driven by the probe and is not observed below the wave-breaking threshold, and is instead driven by the breaking of the short-wavelength wave. From 1D cold-plasma theory, below the wave-breaking threshold, individual electron charge sheets do not cross. The force acting on a sheet therefore depends only on the smeared-out ionic background, leading to simple harmonic motion [4]. When the wave breaks, charge sheets cross and so experience an additional force due to the electron-charge imbalance. Since the point at which the wave breaks travels with the probe, the associated plasma excitation has a phase velocity $\sim c$, resulting in a long-wavelength excitation.

A similar effect has been identified in low-density plasma, in which the excitation arises from ponderomotive nonlinearity, and has been suggested as a method to allow controlled electron acceleration with relatively low-intensity pulses [17]. The effect observed here has the potential advantage that higher-density plasma may be used, allowing a larger accelerating field. Further, there is no constraint on the probe duration, making the effect more widely accessible; for a sufficiently intense pump, the only requirement is that the integrated probe amplitude is sufficiently high for wave breaking to occur.

III. ANALYTICAL MODEL

The decrease in the effective probe amplitude caused by self-steepening is comparable to the effect of shadowing [18], in which the leading edge of the probe is preferentially amplified, lowering the effective seeding power. The effect here, however, is distinct, as wave breaking changes the interaction, preventing the π-pulse solution which arises in the pump-depletion regime [3]. To illustrate this, we consider the coupled three-wave equations widely used in the study of parametric amplification. Phenomenological treatments for wave breaking in the three-wave model have been investigated in other works [6,19], as have three-wave models incorporating damping and frequency shifts calculated from a nonlinear density distribution function [20]. Rather than attempting to derive the exact behavior of the system in regimes far above the wave-breaking threshold, we find that using only simple assumptions we can recover the qualitative behavior observed in Fig. 1. We note that although dispersion plays a role towards the end of the simulation in Fig. 1, amplification remains the dominant process until the end of the pump-probe interaction. We therefore limit ourselves to the linearized, dispersion-free equations for pump, probe, and plasma wave, to obtain the following:

$$(\partial_t - \partial_z)a = \frac{i}{2\omega_a}\tilde{\psi}^* b, \quad (\partial_t + \partial_z)b = \frac{i}{2\omega_b}\tilde{\psi} a,$$
$$(\partial_t + \Omega)\tilde{\psi} = \frac{i\omega_p\omega_a^2}{2} a^* b. \tag{1}$$

Here a and b are the envelopes of the pump and probe, respectively, which satisfy $\vec{a} = \Re\mathfrak{e}([a\,e^{i\phi_a} + b\,e^{i\phi_b})\vec{u}]$, with $\vec{a}$

the reduced vector potential, $\phi_{a,b} = \omega_{a,b}(t \pm z/c)$ the carrier phases of the pump and probe, and $\vec{u}$ the polarization vector, $\vec{u} = (\hat{x} + i\hat{y})/\sqrt{2}$ for circularly polarized light. We retain the coupling susceptibility, $\tilde{\psi} = < (ne^2/\varepsilon_0 \gamma m)\, e^{i(\phi_a - \phi_b)} >$, which is related to the normalized electric field used in, e.g., Ref. [3], by $\tilde{\psi} = 2i\omega_a\omega_p f^*$. The functional $\Omega[x,t,\tilde{\psi}]$ allows the effects of wave breaking to be taken into account. Assuming an initially cold plasma, valid for the low temperatures considered here, we expect no influence from wave breaking below the threshold $\psi_{\rm br} = 0.5\omega_p^2$, which yields

$$\Omega[x,t,\tilde{\psi}] = \begin{cases} 0, & \max\limits_{0\leqslant t'\leqslant t}(|\tilde{\psi}(x,t')|) \leqslant \tilde{\psi}_{\rm br}, \\ \nu + i\delta, & \max\limits_{0\leqslant t'\leqslant t}(|\tilde{\psi}(|x,t')|) > \psi_{\rm br}, \end{cases} \tag{2}$$

where ν and δ are the damping rate and shift in the resonant frequency of the plasma wave due to wave breaking (in a full treatment, these quantities will certainly vary in time).

Assuming the probe is sufficiently intense for wave breaking to occur (readily satisfied for high pump intensities), the analytical π-pulse solution for the pump-depletion regime will remain valid only for the leading edge of the interaction, before the wave breaks. Substituting the wave-breaking threshold for $\tilde{\psi}$ into these equations, we obtain the pump amplitude at wave breaking, $a_{\rm br} = [a_0^2 - (\omega_p/2\omega_a)^3]^{1/2}$. We note that $a_{\rm br}$ is independent of the initial probe amplitude. Moreover, we find that the pump depletion at wave breaking, $\sim a_0^2 - a_{\rm br}^2 = (\omega_p/2\omega_a)^3$, is independent of both pump and probe amplitudes and corresponds to the threshold pump intensity for wave breaking to occur.

The energy density of the plasma wave at wave breaking depends only on its frequency and wave number. Since the pump depletion is fixed, it follows that the intensity increase of the probe up to wave breaking is also independent of the laser amplitudes. Either the probe growth rate is high, in which case wave breaking occurs rapidly, or the growth rate is low, and wave breaking occurs proportionally later. The energy gain can be modified only by changing the laser and plasma frequencies, which alters the energy partition and the wave-breaking threshold, or by changing the interaction volume, i.e., a longer pump or wider-diameter beams.

Therefore, in order to improve amplification, we must consider the interaction after wave breaking. As the plasma electrons move with finite velocity, $\tilde{\psi}$ must be continuous in time, and so Ω must remain finite. Since the damping and the shift in resonance arise due to phase mixing within the broken wave, we expect the characteristic decay time of the wave to be of the order $1/\omega_p$. In the finite time for coupling to break down after wave breaking, we therefore find the total energy transfer will be greater for larger pump and probe amplitudes.

Put simply, the energy transfer prior to wave breaking is independent of the laser amplitudes, and so efficient amplification relies on maximizing the energy transfer after the wave has broken. This is achieved by maximizing the probe amplitude in the period immediately after wave breaking, before phase mixing destroys the coupling between pump and probe, which requires high-contrast probe pulses of duration $\sim 1/\omega_p$.

The "soft-wave-breaking" model discussed by Balakin [6], in which wave breaking limits but does not reduce the probe growth, can be considered as equivalent to this model in the limit of very low plasma density, where the probe duration is $\ll 1/\omega_p$. The model discussed here, however, remains valid for the higher plasma densities necessary for significant amplification.

We therefore make a distinction between the wave-breaking regime [11], in which amplification of a long probe is significantly reduced by phase mixing after the plasma wave breaks, and the coherent wave-breaking (CWB) regime, observed for the shortest pulse in Fig. 1, in which the probe is sufficiently short that the probe peak is amplified, even after the wave breaks. The CWB regime is therefore characterized by much higher efficiencies than the wave-breaking regime, and so the use of a high-quality probe pulse, with short duration and good contrast ratio, is vital for experimental campaigns.

IV. APPLICABILITY TO EXPERIMENTS

To illustrate this importance, Fig. 3 shows the pump-to-probe energy-transfer efficiency while varying the pump intensity for different initial probe durations. Only energy transferred to the probe within 500 fs the initial probe peak is considered. Other parameters are as for Fig. 1. Using a shorter pulse gives rise to higher efficiencies over a wide range of pump intensities beyond the wave-breaking threshold. Despite this, better efficiencies are achieved by using a pump below the wave-breaking threshold. In this regime, longer probe pulses exhibit higher efficiencies, as the more energetic probe is better able to deplete the pump.

Although below-wave-breaking amplification yields higher efficiencies, this regime is not necessarily preferable for experiments, as the large interaction volumes required for the same total pump energy may be technically difficult to achieve. Physically, changing the pump intensity while keeping the probe constant, as is the case for Fig. 3, can be understood as the effect of stretching the pump in time; the same total energy for a 1×10^{13} W cm^{-2} pump would therefore require a 45 cm interaction length. For limited interaction volumes, then, a higher intensity pump may be preferable in order to maximize energy transfer, despite the decrease in efficiency. With these considerations in mind, the use of a shorter probe pulse becomes important in order to access the the CWB regime. This regime has the additional advantage that the

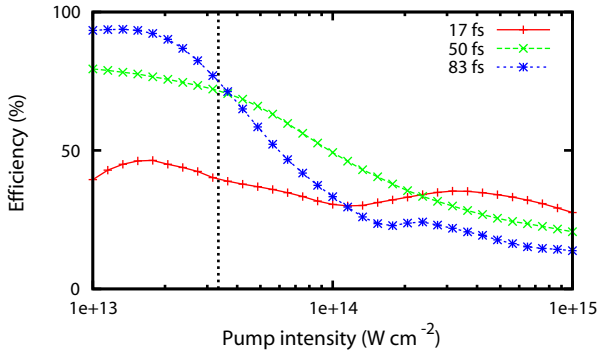

FIG. 3. (Color online) Pump-to-probe energy-transfer efficiency for varying pump intensity. The vertical dashed line shows the wave-breaking threshold.

duration of the amplified probe can also be significantly shorter than that achieved at lower pump intensities.

Although the ∼95% efficiency observed at low pump intensity is more than one order of magnitude better than the best experimental results to date, we note that no experiments have been carried out with similar parameters: Ren *et al.* [10] used an initial probe intensity $\sim 10^{12}$ W cm^{-2}, compared to the 1×10^{16} W cm^{-2} used here. We note, however, that the low efficiencies observed in recent campaigns at petawatt-scale facilities (Vulcan, PHELIX) may be due to the lack of a suitable probe, as the shortest available pulses at such facilities are often $\gg$100 fs duration.

Multidimensional simulations show that for beams with Gaussian transverse profiles, the optimal probe duration for a given pump intensity tends to be longer than that shown here, although the general trends are the same. This is due to the fact that at larger radii, the pump and probe intensities are lower, and so while the center of the interaction may be far beyond wave breaking, some parts of the interaction will be in the near-wave-breaking or below-wave-breaking regimes, for which longer probe durations are preferable. As each regime has different requirements for optimal efficiency, purpose-built Raman amplifiers would likely benefit from the use of flat-top profile beams, as the optimal probe parameters are the same for all radii.

V. CONCLUSIONS

To conclude, we identify the coherent wave-breaking (CWB) regime of Raman amplification, in which significant amplification occurs after the onset of wave breaking. The regime is accessed by using a short, intense probe pulse, which results in wave breaking occurring close to the peak of the amplified probe, maximizing the energy transfer from pump to probe in the time before significant phase mixing occurs. This regime is of great importance to achieving high amplification, as experimental constraints act to limit the possible interaction volume and as such limit the possible energy transfer that can be attained below the wave-breaking threshold.

ACKNOWLEDGMENTS

This work was funded by DFG TR18, EU FP7, EuCARD^2, and BMBF.

[1] G. Shvets, N. J. Fisch, A. Pukhov, and J. Meyer-ter-Vehn, Superradiant Amplification of an Ultrashort Laser Pulse in a Plasma by a Counterpropagating Pump, Phys. Rev. Lett. **81**, 4879 (1998).

[2] R. M. G. M. Trines, F. Fiuza, R. Bingham, R. A. Fonseca, L. O. Silva, R. A. Cairns, and P. A. Norreys, Simulations of efficient Raman amplification into the multipetawatt regime, Nat. Phys. **7**, 87 (2011).

[3] V. M. Malkin, G. Shvets, and N. J. Fisch, Fast Compression of Laser Beams to Highly Overcritical Powers, Phys. Rev. Lett. **82**, 4448 (1999).

[4] J. M. Dawson, Nonlinear electron oscillations in a cold plasma, Phys. Rev. **113**, 383 (1959).

[5] N. A. Yampolsky, N. J. Fisch, V. M. Malkin, E. J. Valeo, R. Lindberg, J. Wurtele, J. Ren, S. Li, A. Morozov, and S. Suckewer, Demonstration of detuning and wavebreaking effects on Raman amplification efficiency in plasma, Phys. Plasmas **15**, 113104 (2008).

[6] A. Balakin, D. Kartashov, A. Kiselev, S. Skobelev, A. Stepanov, and G. Fraiman, Laser pulse amplification upon Raman backscattering in plasma produced in dielectric capillaries, JETP Lett. **80**, 12 (2004).

[7] W. Cheng, Y. Avitzour, Y. Ping, S. Suckewer, N. J. Fisch, M. S. Hur, and J. S. Wurtele, Reaching the Nonlinear Regime of Raman Amplification of Ultrashort Laser Pulses, Phys. Rev. Lett. **94**, 045003 (2005).

[8] C.-H. Pai, M.-W. Lin, L.-C. Ha, S.-T. Huang, Y.-C. Tsou, H.-H. Chu, J.-Y. Lin, J. Wang, and S.-Y. Chen, Backward Raman Amplification in a Plasma Waveguide, Phys. Rev. Lett. **101**, 065005 (2008).

[9] G. Vieux, A. Lyachev, X. Yang, B. Ersfeld, J. P. Farmer, E. Brunetti, R. C. Issac, G. Raj, G. H. Welsh, S. M. Wiggins, and D. A. Jaroszynski, Chirped pulse Raman amplification in plasma, New J. Phys. **13**, 063042 (2011).

[10] J. Ren, W. Cheng, S. Li, and S. Suckewer, A new method for generating ultraintense and ultrashort laser pulses, Nat. Phys. **3**, 732 (2007).

[11] Z. Toroker, V. M. Malkin, and N. J. Fisch, Backward Raman amplification in the Langmuir wavebreaking regime, Phys. Plasmas **21**, 113110 (2014).

[12] M. R. Edwards, Z. Toroker, J. M. Mikhailova, and N. J. Fisch, The efficiency of Raman amplification in the wavebreaking regime, Phys. Plasmas **22**, 074501 (2015).

[13] J. P. Farmer and A. Pukhov, Fast multidimensional model for the simulation of Raman amplification in plasma, Phys. Rev. E **88**, 063104 (2013).

[14] J. P. Farmer and A. Pukhov, Applicability of the envelope model, Proc. SPIE **9509**, 95090H (2015).

[15] B. Ersfeld and D. A. Jaroszynski, Superradiant Linear Raman Amplification in Plasma Using a Chirped Pump Pulse, Phys. Rev. Lett. **95**, 165002 (2005).

[16] Y. A. Tsidulko, V. M. Malkin, and N. J. Fisch, Suppression of Superluminous Precursors in High-Power Backward Raman Amplifiers, Phys. Rev. Lett. **88**, 235004 (2002).

[17] G. Shvets, N. J. Fisch, A. Pukhov, and J. Meyer-ter-Vehn, Generation of periodic accelerating structures in plasma by colliding laser pulses, Phys. Rev. E **60**, 2218 (1999).

[18] N. A. Yampolsky, V. M. Malkin, and N. J. Fisch, Finite-duration seeding effects in powerful backward Raman amplifiers, Phys. Rev. E **69**, 036401 (2004).

[19] J. P. Farmer, B. Ersfeld, and D. A. Jaroszynski, Raman amplification in plasma: Wavebreaking and heating effects, Phys. Plasmas **17**, 113301 (2010).

[20] R. R. Lindberg, A. E. Charman, and J. S. Wurtele, Reduced kinetic description of weakly-driven plasma waves, Phys. Plasmas **15**, 055911 (2008).